Quantum spin state selectivity and magnetic tuning of ultracold chemical reactions of triplet alkali-metal dimers with alkali-metal atoms

Rebekah Hermsmeier[1], Jacek Kłos[2,3], Svetlana Kotochigova[3] and Timur V. Tscherbul[1]
[1]*Department of Physics, University of Nevada, Reno, NV, 89557, USA*
[2]*Department of Physics, Joint Quantum Institute, University of Maryland College Park, College Park, Maryland, 20742, USA*
[3]*Department of Physics, Temple University, Philadelphia, PA 19122, USA*
(Dated: August 2, 2021)

We demonstrate that it is possible to efficiently control ultracold chemical reactions of alkali-metal atoms colliding with open-shell alkali-metal dimers in their metastable triplet states by choosing the internal hyperfine and rovibrational states of the reactants as well as by inducing magnetic Feshbach resonances with an external magnetic field. We base these conclusions on coupled-channel statistical calculations that include the effects of hyperfine contact and magnetic-field-induced Zeeman interactions on ultracold chemical reactions of hyperfine-resolved ground-state Na and the triplet NaLi($a^3\Sigma^+$) producing singlet $Na_2(^1\Sigma_g^+)$ and a Li atom. We find that the reaction rates are sensitive to the initial hyperfine states of the reactants. The chemical reaction of fully spin-polarized, high-spin states of rotationless NaLi($a^3\Sigma^+, v = 0, N = 0$) molecules with fully spin-polarized Na is suppressed by a factor of 10-100 compared to that of unpolarized reactants. We interpret these findings within the adiabatic state model, which treats the reaction as a sequence of nonadiabatic transitions between the initial non-reactive high-spin state and the final low-spin states of the reaction complex. In addition, we show that magnetic Feshbach resonances can similarly change reaction rate coefficients by several orders of magnitude. Some of these resonances are due to resonant trimer bound states dissociating to the $N = 2$ rotational state of NaLi($a^3\Sigma^+, v = 0$) and would thus exist in systems without hyperfine interactions.

Introduction. Recent experimental advances in molecular cooling and trapping have opened up new avenues of research into controlling chemical reactivity with external electromagnetic fields [1–3], the idea that fascinated scientists for decades, and led to the development of new research frontiers at the interface of chemistry and physics, such as mode-selective chemistry [4, 5], quantum coherent control [6], and attochemistry [7]. In particular, the production and trapping of ground-state molecular radicals NaLi($a^3\Sigma^+$), $Li_2(a^3\Sigma^+)$, $Rb_2(a^3\Sigma^+)$, SrF($^2\Sigma^+$), CaF($^2\Sigma^+$), YO($^2\Sigma^+$), YbF($^2\Sigma^+$) [8–14] and studies of their collisional properties at μK temperatures [15–18] suggested the possibility of using the reactants's electron spin degrees of freedom to tune ultracold reaction dynamics by magnetic fields.

The prospect of using magnetic fields as a tool to control chemical reactivity is central to ultracold chemistry [1, 2] and a very important one in chemical kinetics [19] and biological magnetoreception [20], where radical pair reactions in cryptochrome proteins are thought to play a key role in magnetic-field-guided orientation of birds and insects [21, 22]. However, despite the long-standing significance of this question and the recent experimental observations of inelastic collisions in an ultracold Na-NaLi($a^3\Sigma^+$) mixture [18], no theoretical studies have been reported on ultracold reaction dynamics involving ground-state alkali-metal dimers and atoms in the presence of external magnetic fields and hyperfine interactions. This is because such reactions occur through the formation of a deeply bound reaction complex [23–25], whose numerous strongly coupled bound and resonance states defy rigorous quantum scattering calculations [24–26].

Here, we explore the dynamics of the ultracold chemical reaction Na + NaLi($a^3\Sigma^+$) $\rightarrow$ $Na_2(^1\Sigma_g^+)$ + Li in the presence of magnetic fields and hyperfine interactions using the extended coupled-channel statistical (CCS) model [27] parametrized by *ab initio* calculations. The model assumes the existence of a long-lived reaction complex at short range, whose properties can be modeled statistically (*i.e.* using classical probabilities) [28–30]. Statistical (or universal) models [28–42] have been successfully applied to calculate the rate of ultracold chemical reactions of alkali-metal dimers [32, 34–36, 39] and the density of states of the $(KRb)_2$ reaction complex [43]. However, the previous calculations have been limited to the case of zero magnetic field and did not account for electron spins, hyperfine interactions, and non-adiabatic effects, all of which we will consider in the present work.

Our calculations show that the fully spin-polarized spin states of NaLi and Na are ∼10-100 times less chemically reactive than unpolarized spin states, demonstrating extensive quantum spin state control of chemical reactions of triplet-state alkali-metal dimers with alkali-metal atoms. We also find that the magnetic field dependence of the reaction rate displays several magnetic Feshbach resonances (MFRs), providing the first theoretical prediction of MFRs in an ultracold chemical reaction. MFRs in non-reactive scattering of NaK with K were observed experimentally and thoroughly analysed in Refs. [44–46]. Our findings open up several new avenues of research in ultracold molecular physics and chemistry. The reactive MFRs will enable experimentalists to efficiently suppress unwanted chemical reactivity in trapped atom-molecule mixtures, enabling, e.g., effi-

cient sympathetic cooling [18, 47–52]. They could also be used to assemble chemically reactive atom-molecule trimers via magnetoassociation, to engineer entangled many-body states in trapped atom-molecule mixtures, and to probe and control the quantum dynamics of chaotic scattering and reaction complex formation [24].

Theory: Ab initio calculations and extended CCS model. To describe ultracold reactive collisions between Na atoms and NaLi molecules in the metastable $a^3\Sigma^+$ electronic state, we performed *ab initio* calculations of the electronic potential energy surfaces (PESs) of the long-lived intermediate Na_2Li reaction complex. The complex is characterized by two $^2A'$ and one $^4A'$ trimer electronic states. The potential landscape of these barrierless PESs is shown in Fig. 1. The PESs are expressed in the Jacobi coordinates $\mathbf{R}$—the atom-molecule separation vector and $\mathbf{r}$—the vector joining the nuclei of the diatomic molecule. For our purposes it is sufficient to determine the PESs, which are only functions of R and θ (the angle between $\mathbf{R}$ and $\mathbf{r}$) in the two-dimensional plane with the internuclear distance of NaLi fixed at its equilibrium value ($r = r_e$) [27]. Our *ab initio* calculations of the two-state $^2A'$ PESs reveal a conical intersection (CI) between the two doublet states which is located at $R \simeq 8.5a_0$ and $\theta = 70^o$. The relevant multi-dimensional PESs have been determined using the internally-contracted multi-reference configuration interaction (MRCI) method [53] with single and double excitations and Davidson correction [54] as further described in the Supplemental Material [55].

From the energetics of the relevant molecular states in the entrance and exit reaction channels we determine that the production of the $Na_2(a^3\Sigma_u^+)$ molecule in the $Na(^2S)$ + $NaLi(a^3\Sigma^+)$ reaction is endothermic by 41.7 cm^{-1} including the zero-point vibrational energy correction. This suggests that the vibrational excitation of the reactant $NaLi(a^3\Sigma^+)$ molecule to the $v \geq 2$ vibrational states will allow for production of triplet-state Na_2 products. However, the CI allows for an efficient transfer of the reactant $NaLi(a^3\Sigma^+)$ molecules into either NaLi $(X^1\Sigma^+)$ or $Na_2(X^1\Sigma_g^+)$ states of the ground electronic configuration. A schematic depiction of reactive scattering between Na atoms and $NaLi(a^3\Sigma^+)$ molecules through a CI is demonstrated in Fig. 1(a). The reactants start out on the asymptotically degenerate $2^2A'$ and $1^4A'$ excited PESs. The reaction flux on the $2^2A'$ PESs can reach the CI and make a transition to the ground $1^2A'$ PES leading to ground-state reaction products. Only the $2^2A'$ and $1^4A'$ PESs are included in our CCS calculations, which is justified by the fact that the CI is located deeply inside the reaction complex region not explicitly included in the calculations [55].

The extended CCS model of barrierless chemical reactions [27] assumes the existence of a long-lived reaction complex, whose formation from the reactants or decay to products can be treated as independent events [28, 29]. The state-to-state reaction probability between the reactant and product states r and p

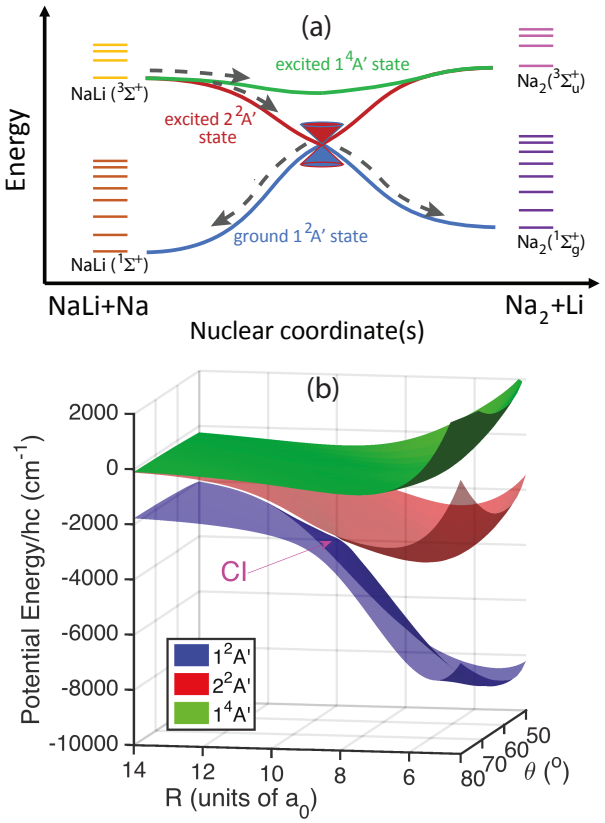

FIG. 1. (a) Schematic of the Na + $NaLi(a^3\Sigma^+)$ reactive scattering through a CI between the $^2A'$ PESs leading to either ground state $NaLi(X^1\Sigma^+)$ or $Na_2(X^1\Sigma_g^+)$ molecules. The CI is indicated by the red/blue cone. (b) *Ab initio* adiabatic PESs for Na-NaLi as functions of the Na-to-NaLi separation R and of the bending angle θ with $r = 9.1a_0$, close to the equilibrium distance of the $NaLi(a^3\Sigma^+)$ potential. The blue ($1^2A'$) and red ($2^2A'$) PESs have a CI, where two PESs of the same electronic symmetry touch. The green surface is the spin-polarized, nonreactive PES of the $1^4A'$ symmetry.

$P_{r\to p}(E) = \frac{p_p(E)p_r(E)}{\sum_c p_c(E)}$, where $p_r(E)$ and $p_p(E)$ are the energy-dependent capture probabilities of the reactants and products into the reaction complex obtained by solving the time-independent Schrödinger equation in the entrance reaction channel subject to a short-range capture boundary condition for the reactive $2^2A'$ PES and a regular boundary condition for the nonreactive $^4A'$ PES [27, 55].

Ultracold reaction dynamics in a magnetic field. We begin by describing the hyperfine energy level structure of the reactants in a magnetic field. Figures 2(b) and (c) show the Zeeman levels of Na and $NaLi(a^3\Sigma^+, v = 0, N = 0)$ obtained by diagonalization of the atomic and molecular Hamiltonians [55]. There are a total of 36 molecular energy levels in the $N = 0$ manifold of $NaLi(a^3\Sigma^+)$, which can be classified in the weak-field limit by the values of the total angular momentum of the molecule F and its projection on the field axis M_F [68, 69]. The calculated zero-field hyperfine splittings

are in good agreement with the measured values [8, 55].

To explore the influence of reactant spin polarization on chemical reactivity, we consider reactive collisions of NaLi molecules in the highest-energy level $|36\rangle$ of the $N = 0$ manifold with Na atoms in the hyperfine states $|7\rangle$ and $|8\rangle$ [see Figs. 2(b) and (c)]. Note that state $|36\rangle$ is a triply spin-polarized state of NaLi, where all of the spins in the molecule are aligned along the magnetic field. Similarly, state $|8\rangle$ of Na is doubly spin-polarized ($|F = 2, m_F = 2\rangle$), in contrast to state $|7\rangle$. In the absence of the hyperfine structure, the Zeeman states of NaLi and Na shown in Fig. 2 reduce to 3 molecular states $|S_A M_{S_A}\rangle$ ($M_{S_A} = 0, \pm 1$), and 2 atomic states $|S_B M_{S_B}\rangle$ ($M_{S_B} = \pm 1/2$). The fully spin-polarized initial states of Na and NaLi are labeled as $|2\rangle$ and $|3\rangle$.

In Fig. 2(a) we plot the magnetic field dependence of the reaction rates for the (8,36) and (7,36) initial states of Na + NaLi($a^3\Sigma$) at $T = 2$ μK. The rates are nearly temperature independent, as expected for a two-body inelastic process near an s-wave threshold [70].

More significantly, we observe that the chemical reactivity of fully spin-polarized reactants Na(8) + NaLi(36) is suppressed by a factor of $\simeq$10-100 compared to that of non-fully spin-polarized reactants Na(7) + NaLi(36). Remarkably, flipping the electron spin of one of the reactants leads to a dramatic change in chemical reactivity. While the strong dependence on the initial spin state has been observed previously for Penning ionization in cold atom-atom collisions [71], the atom-molecule reaction studied here is essentially different due to the large number of participating rovibrational states coupled by strongly anisotropic atom-molecule interactions.

The rate of the Na(7) + NaLi(36) reaction displays the opposite trend, beginning to decrease at $B \geq 0.05$ T. This trend is similar to that observed in [27] and can be explained by referring to Eq. (1): the weight $c_2(B)$ of the "reactive" electron spin state $|\frac{1}{2}, -\frac{1}{2}\rangle$ in the hyperfine state $|7\rangle$ of Na

$$|7\rangle = c_1(B)|\tfrac{1}{2}\tfrac{1}{2}\rangle|\tfrac{3}{2}\tfrac{1}{2}\rangle + c_2(B)|\tfrac{1}{2}, -\tfrac{1}{2}\rangle|\tfrac{3}{2}\tfrac{3}{2}\rangle \qquad (1)$$

decreases with increasing magnetic field, as the state tends to the unreactive spin-polarized state $|\frac{1}{2}\frac{1}{2}\rangle|\frac{3}{2}\frac{1}{2}\rangle$ in the large-field limit (where $|\frac{1}{2}\frac{1}{2}\rangle|\frac{3}{2}\frac{1}{2}\rangle$ denotes the Zeeman state with $S_B = M_{S_B} = \frac{1}{2}$, $I_B = \frac{3}{2}$, and $M_{I_B} = \frac{1}{2}$). The hyperfine state $|7\rangle$ of Na becomes less and less reactive towards NaLi with increasing field because the reactive weight $c_2(B) \simeq B^{-1}$ [27]. We note that the spin-polarized reaction rates calculated with and without the hyperfine structure of Na and NaLi taken into account [see Fig. 2(a)] are similar in magnitude and field dependence. The fully spin-stretched hyperfine states $|36\rangle$ of NaLi and $|8\rangle$ of Na are direct products of the electron and nuclear spin states, so the nuclear spin degree of freedom only causes a slight shift in threshold energies, but otherwise plays the role of a spectator.

The suppression of chemical reactivity of spin-polarized molecules is due to a general mechanism [72–74] based on approximate conservation of the total spin

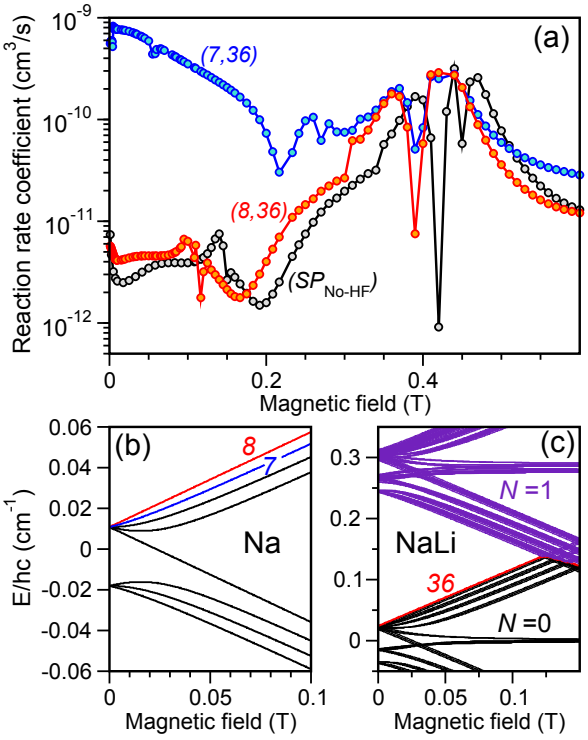

FIG. 2. (a) Magnetic-field dependence of the reaction rate coefficient for the fully spin-polarized Na(8) + NaLi(36) [red curve with label (8,36)] and non-fully spin polarized Na(7) + NaLi(36) collisions [blue curve]. Also shown are results [black curve labeled by $SP_{\mathrm{No-HF}}$] for calculations where the hyperfine contact interactions are turned off. Here, the initial state is the spin-polarized Na($|S_B, M_{S_B} = 1/2, 1/2\rangle$) + NaLi($|S_A, M_{S_A} = 1, 1\rangle$) state. The collision energy is $E/k = 2$ μK for all data. Here, k is the Boltzmann constant. Panel (b) shows the hyperfine and Zeeman energy levels of the ground-state Na atom. Panel (c) shows the rotational, hyperfine, and Zeeman energy levels of the $N = 0$ and 1 rotational states of NaLi($a^3\Sigma^+, v = 0$). In panels (b) and (c) relevant hyperfine states (blue and red colored curves) are indexed as $1, 2, 3, \ldots$ in the order of increasing energy.

of the reaction complex. Specifically, if the electron spins of the reactants are completely polarized, the reaction complex is initialized in the nonreactive state of total spin $S = 3/2$ described by the $^4A'$ PES (see Fig. 1). Thus, in the absence of S-nonconserving interactions, such as the intramolecular spin-spin or intermolecular magnetic dipole interactions, the value of S must be the same for the reactants and products (the Wigner spin rule [72]). The energetically allowed products of the Na + NaLi reaction—molecular $Na_2(^1\Sigma_g^+)$ and atomic $Li(^2S_{1/2})$—correspond to $S = 1/2$. As a result, the spin-polarized chemical reaction Na + NaLi($a^3\Sigma^+$) $\rightarrow$ $Na_2(^1\Sigma_g^+)$ + Li requires spin-changing intersystem crossing transition $S = 3/2 \rightarrow 1/2$ [75–79] in order to proceed. We verified that omitting the spin-spin and magnetic dipolar interactions from CCS calculations leads to a complete suppression of the reaction Na(8) + NaLi(36) $\rightarrow$ Na_2 + Li, while having little ef-

fect on the reactivity of the initial state (7,36).

To gain further insight into the mechanism of the spin-polarized chemical reaction Na + NaLi($a^3\Sigma^+$) we plot in Fig. 3(a) the adiabatic eigenvalues $\epsilon_i(R)$ of the atom-molecule Hamiltonian [31, 33, 80–82]. Consider, e.g., the $S = 3/2$ diabatic potential obtained by following the corresponding adiabatic curves through a series of avoided crossings shown in Fig. 3. The potential is repulsive at short range with a well depth of $\simeq$ 200 cm^{-1}, and correlates with the fully spin-polarized initial state of Na(2)-NaLi(3). The repulsive state experiences several crossings with the $S = 1/2$ diabatic states, which are attractive at short range and correlate asymptotically with unpolarized rotationally excited states of NaLi. The crossings are induced by S-nonconserving interactions, predominantly by the intramolecular spin-spin interaction of NaLi($a^3\Sigma$), which cause the chemical reaction. We note that a simple two-channel model involving the pair of diabatic states near the largest avoided crossing shown in Fig. 3(b) underestimates the reaction rate by several orders of magnitude (as does Landau-Zener theory), suggesting the importance of multichannel effects.

The resonance variation of the spin-polarized reaction rate near $B = 0.4$ T shown in Fig. 2(a) is caused by MFRs, which occur due to the coupling of the incident spin-polarized channel $|N_A = 0, M_{S_A} = 1\rangle$ with closed-channel bound states $|N'_A = 2, M'_{S_A}\rangle$ ($M'_{S_A} \neq M_{S_A}$) mediated by *anisotropic interactions*, which include the intramolecular spin-spin interaction of NaLi($a^3\Sigma^+$) [83] and the anisotropic part of the Na-NaLi interaction. The near-threshold bound state responsible for the MFR at 0.42 T is supported by the adiabatic potential that correlates to the $|N'_A = 2, M'_{S_A} = 0\rangle|M'_{S_B} = -\frac{1}{2}\rangle$ closed-channel threshold, as shown in Fig. 3(c).

Figure 3(e) illustrates that MFRs can also occur in the spin-unpolarized incident channel (1,3). The low-field resonance is mainly due to the atom-molecule interaction anisotropy, which couples the $N = 0$ incident channel with $N > 0$ closed channels. Indeed, as shown in Fig. 3(e) the MFR disappears when the anisotropic part of the Na-NaLi interaction is omitted.

Our calculated Na-NaLi reaction rates deviate substantially from the universal value $k_0^u = 1.84 \times 10^{-10}$ cm^3/s [84, 85] calculated using the accurate *ab initio* Na-NaLi($a^3\Sigma^+$) long-range dispersion coefficient $C_6 =$ 4026 a.u. [55]. This indicates a substantial degree of non-universality due to the inherently multichannel nature of the reaction dynamics caused by anisotropic interactions (see above). As shown in Fig. 3(a) a large fraction of adiabatic channels, through which the reaction occurs, is repulsive at short range, leading to a significant reflection of the incident flux even for unpolarized initial reactant states. This reflection manifests in the appearance of MFRs and other non-universal effects [84]. Test calculations show that in the absence of anisotropic interactions, the unpolarized reaction rate remains close to the universal limit over the entire range of magnetic fields [see Fig. 3(e)].

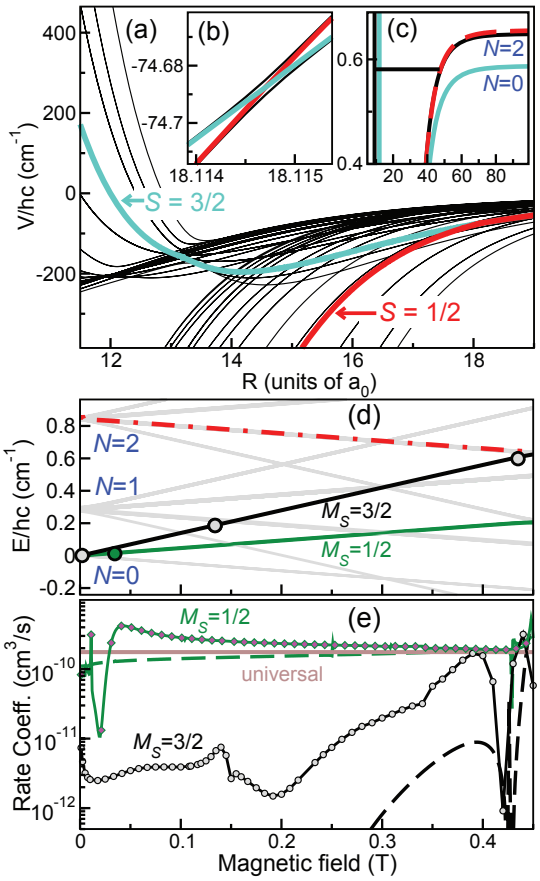

FIG. 3. (a) Adiabatic potentials (thin black curves) of the Na-NaLi reaction complex in the absence of the hyperfine contact interactions at $B = 0.01$ T and $M = 3/2$. Diabatized potentials for $S = 1/2$ and $3/2$ are shown as cyan and red curves, respectively. (b) A blowup of the avoided crossing near $18.1a_0$; (c) Open-channel (cyan curve) and closed-channel (black and red dashed curves) diabatic potentials near the $N = 0$ and 2 NaLi rotational thresholds at $B = 0.42$ T. The closed-channel bound state is shown by the horizontal bar. (d) Threshold energies (grey curves) of Na+NaLi as functions of magnetic field. Our incident thresholds labeled $M_S = 1/2$ and $M_S = 3/2$ are colored as green and black curves, respectively ($M_S = M_{S_A} + M_{S_B}$). The $|N_A = 2, M_{N_A} = -1, M_{S_A} = 0\rangle|M_{S_B} = -\frac{1}{2}\rangle$ closed-channel threshold is the dashed red curve; (e) Na + NaLi reaction rate coefficients for the spin-polarized $M_S = 3/2$ (circles) and unpolarized $M_S = 1/2$ (diamonds) initial states as functions of magnetic field. Solid and dashed lines correspond to calculations including and excluding the anisotropic part of the Na-NaLi PESs. The universal limit is indicated by the brown horizontal line. Locations of MFRs in this panel and thus of zero-energy closed-channel bound states, are shown as colored circles in panel (d).

In summary, we have presented a theoretical study of the ultracold chemical reaction of Na atoms with triplet NaLi($a^3\Sigma^+$) molecules in their ground rovibrational states in the presence of external magnetic fields and hyperfine interactions. This reaction is representative of a wide class of ultracold chemical reactions of

triplet alkali-dimer molecules currently studied by several experimental groups [15, 16, 18]. Our calculations reveal a substantial degree of quantum state selectivity in the dependence of the reaction rate on the initial states of the reactants (fully spin-polarized vs. unpolarized). Our results also suggest that it is possible to control ultracold chemical reactions of alkali-metal dimers with alkali-metal atoms via magnetic Feshbach resonances. The generality of the spin-based control mechanisms explored here implies their potential utility as a tool to control other, potentially more complex chemical reactions, such as those of heavier bialkali molecules [e.g., K + KRb($a^3\Sigma$)] and those involving $^2\Sigma$ molecules, such as Li + CaH($^2\Sigma$) [27, 48], Li + SrOH($^2\Sigma$) [49], and Li + CaF($^2\Sigma$) [51]. We thus expect our results to be tested in near-future experiments with ultracold atom-molecule mixtures.

We are grateful to Wolfgang Ketterle, Hyungmok Son, Alan Jamison, and Sergey Varganov for stimulating discussions. Work at the University of Nevada, Reno was supported by the NSF Grant No. PHY-1912668. Work at Temple University is supported by the Army Research Office Grant No. W911NF-17-1-0563 and the NSF Grant No. PHY-1908634.

[1] R. V. Krems, Cold controlled chemistry, Phys. Chem. Chem. Phys. **10**, 4079 (2008).
[2] N. Balakrishnan, Perspective: Ultracold molecules and the dawn of cold controlled chemistry, J. Chem. Phys. **145**, 150901 (2016).
[3] J. L. Bohn, A. M. Rey, and J. Ye, Cold molecules: Progress in quantum engineering of chemistry and quantum matter, Science **357**, 1002 (2017).
[4] R. N. Zare, Laser control of chemical reactions, Science **279**, 1875 (1998).
[5] H. Guo and K. Liu, Control of chemical reactivity by transition-state and beyond, Chem. Sci. **7**, 3992 (2016).
[6] M. Shapiro and P. Brumer, *Quantum Control of Molecular Processes* (Wiley-VCH, 2012).
[7] M. Nisoli, P. Decleva, F. Calegari, A. Palacios, and F. Martín, Attosecond electron dynamics in molecules, Chem. Rev. **117**, 10760 (2017).
[8] T. M. Rvachov, H. Son, A. T. Sommer, S. Ebadi, J. J. Park, M. W. Zwierlein, W. Ketterle, and A. O. Jamison, Long-lived ultracold molecules with electric and magnetic dipole moments, Phys. Rev. Lett. **119**, 143001 (2017).
[9] J. F. Barry, D. J. McCarron, E. B. Norrgard, M. H. Steinecker, and D. DeMille, Magneto-optical trapping of a diatomic molecule, Nature (London) **512**, 286 (2014).
[10] D. J. McCarron, M. H. Steinecker, Y. Zhu, and D. DeMille, Magnetic trapping of an ultracold gas of polar molecules, Phys. Rev. Lett. **121**, 013202 (2018).
[11] L. Anderegg, B. L. Augenbraun, Y. Bao, S. Burchesky, L. W. Cheuk, W. Ketterle, and J. M. Doyle, Laser cooling of optically trapped molecules, Nat. Phys. **14**, 890 (2018).
[12] I. Kozyryev, L. Baum, K. Matsuda, B. L. Augenbraun, L. Anderegg, A. P. Sedlack, and J. M. Doyle, Sisyphus laser cooling of a polyatomic molecule, Phys. Rev. Lett. **118**, 173201 (2017).
[13] A. L. Collopy, S. Ding, Y. Wu, I. A. Finneran, L. Anderegg, B. L. Augenbraun, J. M. Doyle, and J. Ye, 3D magneto-optical trap of yttrium monoxide, Phys. Rev. Lett. **121**, 213201 (2018).
[14] J. Lim, J. R. Almond, M. A. Trigatzis, J. A. Devlin, N. J. Fitch, B. E. Sauer, M. R. Tarbutt, and E. A. Hinds, Laser cooled YbF molecules for measuring the electron's electric dipole moment, Phys. Rev. Lett. **120**, 123201 (2018).
[15] B. Drews, M. Deiß, K. Jachymski, Z. Idziaszek, and J. Hecker Denschlag, Inelastic collisions of ultracold triplet Rb_2 molecules in the rovibrational ground state, Nat. Commun. **8**, 14854 (2017).
[16] G. Polovy, E. Frieling, D. Uhland, J. Schmidt, and K. W. Madison, Quantum-state-dependent chemistry of ultracold $^6Li_2$ dimers, Phys. Rev. A **102**, 013310 (2020).
[17] L. W. Cheuk, L. Anderegg, Y. Bao, S. Burchesky, S. S. Yu, W. Ketterle, K.-K. Ni, and J. M. Doyle, Observation of collisions between two ultracold ground-state CaF molecules, Phys. Rev. Lett. **125**, 043401 (2020).
[18] H. Son, J. J. Park, W. Ketterle, and A. O. Jamison, Collisional cooling of ultracold molecules, Nature **580**, 197 (2020).
[19] U. E. Steiner and T. Ulrich, Magnetic field effects in chemical kinetics and related phenomena, Chem. Rev. **89**, 51 (1989).
[20] P. J. Hore and H. Mouritsen, The radical-pair mechanism of magnetoreception, Annu. Rev. Biophys. **45**, 299 (2016).
[21] H. G. Hiscock, S. Worster, D. R. Kattnig, C. Steers, Y. Jin, D. E. Manolopoulos, H. Mouritsen, and P. J. Hore, The quantum needle of the avian magnetic compass, Proc. Natl. Acad. Sci. USA **113**, 4634 (2016).
[22] D. Nohr, B. Paulus, R. Rodriguez, A. Okafuji, R. Bittl, E. Schleicher, and S. Weber, Determination of radical–radical distances in light-active proteins and their implication for biological magnetoreception, Angew. Chem. Int. Ed. **56**, 8550 (2017).
[23] S. C. Althorpe and D. C. Clary, Quantum scattering calculations on chemical reactions, Annu. Rev. Phys. Chem. **54**, 493 (2003).
[24] J. F. E. Croft, C. Makrides, M. Li, A. Petrov, B. K. Kendrick, N. Balakrishnan, and S. Kotochigova, Universality and chaoticity in ultracold K + KRb chemical reactions, Nat. Commun. **8**, 15897 (2017).
[25] B. K. Kendrick, H. Li, M. Li, S. Kotochigova, J. F. E. Croft, and N. Balakrishnan, Non-adiabatic quantum interference effects and chaoticity in the ultracold Li + LiNa → Li_2 + Na reaction, Phys. Chem. Chem. Phys. **23**, 5096 (2021).
[26] M. Morita, R. V. Krems, and T. V. Tscherbul, Universal probability distributions of scattering observables in ultracold molecular collisions, Phys. Rev. Lett. **123**, 013401 (2019).
[27] T. V. Tscherbul and J. Kłos, Magnetic tuning of ultracold barrierless chemical reactions, Phys. Rev. Research **2**, 013117 (2020).
[28] E. J. Rackham, T. Gonzalez-Lezana, and D. E.

Manolopoulos, A rigorous test of the statistical model for atom-diatom insertion reactions, J. Chem. Phys. **119**, 12895 (2003).
[29] M. H. Alexander, E. J. Rackham, and D. E. Manolopoulos, Product multiplet branching in the $O(^1D) + H_2 \rightarrow OH(^2\Pi) + H$ reaction, J. Chem. Phys. **121**, 5221 (2004).
[30] J. F. E. Croft and J. L. Bohn, Long-lived complexes and chaos in ultracold molecular collisions, Phys. Rev. A **89**, 012714 (2014).
[31] D. C. Clary, Fast chemical reactions: Theory challenges experiment, Annu. Rev. Phys. Chem. **41**, 61 (1990).
[32] G. Quéméner and J. L. Bohn, Strong dependence of ultracold chemical rates on electric dipole moments, Phys. Rev. A **81**, 022702 (2010).
[33] M. Auzinsh, E. I. Dashevskaya, I. Litvin, E. E. Nikitin, and J. Troe, Mutual Capture of Dipolar Molecules at Low and Very Low Energies. II. Numerical Study, J. Phys. Chem. A **115**, 5027 (2011).
[34] S. Kotochigova, Dispersion interactions and reactive collisions of ultracold polar molecules, New J. Phys. **12**, 073041 (2010).
[35] Z. Idziaszek and P. S. Julienne, Universal rate constants for reactive collisions of ultracold molecules, Phys. Rev. Lett. **104**, 113202 (2010).
[36] B. Gao, Universal model for exoergic bimolecular reactions and inelastic processes, Phys. Rev. Lett. **105**, 263203 (2010).
[37] G. Quéméner and P. S. Julienne, Ultracold molecules under control!, Chem. Rev. **112**, 4949 (2012).
[38] A. A. Buchachenko, A. V. Stolyarov, M. M. Szczęśniak, and G. Chałasiński, Ab initio long-range interaction and adiabatic channel capture model for ultracold reactions between the KRb molecules, J. Chem. Phys. **137**, 114305 (2012).
[39] M. L. González-Martínez, O. Dulieu, P. Larrégaray, and L. Bonnet, Statistical product distributions for ultracold reactions in external fields, Phys. Rev. A **90**, 052716 (2014).
[40] T. V. Tscherbul and A. A. Buchachenko, Adiabatic channel capture theory applied to cold atom–molecule reactions: Li + CaH → LiH + Ca at 1 K, New J. Phys. **17**, 035010 (2015).
[41] M. D. Frye, P. S. Julienne, and J. M. Hutson, Cold atomic and molecular collisions: approaching the universal loss regime, New J. Phys. **17**, 045019 (2015).
[42] D. Yang, J. Huang, X. Hu, D. Xie, and H. Guo, Statistical quantum mechanical approach to diatom–diatom capture dynamics and application to ultracold KRb + KRb reaction, J. Chem. Phys. **152**, 241103 (2020).
[43] Y. Liu, M.-G. Hu, M. A. Nichols, D. D. Grimes, T. Karman, H. Guo, and K.-K. Ni, Photo-excitation of long-lived transient intermediates in ultracold reactions, Nat. Phys. **16**, 1132 (2020).
[44] J. Rui, H. Yang, L. Liu, D.-C. Zhang, Y.-X. Liu, J. Nan, Y.-A. Chen, B. Zhao, and J.-W. Pan, Controlled state-to-state atom-exchange reaction in an ultracold atom–dimer mixture, Nat. Phys. **13**, 699 (2017).
[45] H. Yang, D.-C. Zhang, L. Liu, Y.-X. Liu, J. Nan, B. Zhao, and J.-W. Pan, Observation of magnetically tunable Feshbach resonances in ultracold $^{23}Na^{40}K + {}^{40}K$ collisions, Science **363**, 261 (2019).
[46] X.-Y. Wang, M. D. Frye, Z. Su, J. Can, L. Liu, D.-C. Zhang, G. Yang, J. M. Hutson, B. Zhao, C.-L. Bai, and J.-W. Pan, Magnetic Feshbach resonances in collisions of $^{23}Na^{40}K$ with ^{40}K, arXiv:2103.07130v1 (2021).
[47] M. Lara, J. L. Bohn, D. Potter, P. Soldán, and J. M. Hutson, Ultracold Rb-OH collisions and prospects for sympathetic cooling, Phys. Rev. Lett. **97**, 183201 (2006).
[48] T. V. Tscherbul, J. Kłos, and A. A. Buchachenko, Ultracold spin-polarized mixtures of $^2\Sigma$ molecules with S-state atoms: Collisional stability and implications for sympathetic cooling, Phys. Rev. A **84**, 040701 (2011).
[49] M. Morita, J. Kłos, A. A. Buchachenko, and T. V. Tscherbul, Cold collisions of heavy $^2\Sigma$ molecules with alkali-metal atoms in a magnetic field: Ab initio analysis and prospects for sympathetic cooling of $SrOH(^2\Sigma^+)$ by $Li(^2S)$, Phys. Rev. A **95**, 063421 (2017).
[50] M. Morita, M. B. Kosicki, P. S. Żuchowski, and T. V. Tscherbul, Atom-molecule collisions, spin relaxation, and sympathetic cooling in an ultracold spin-polarized $Rb(^2S) - SrF(^2\Sigma^+)$ mixture, Phys. Rev. A **98**, 042702 (2018).
[51] M. D. Frye, M. Morita, C. L. Vaillant, D. G. Green, and J. M. Hutson, Approach to chaos in ultracold atomic and molecular physics: Statistics of near-threshold bound states for Li + CaH and Li + CaF, Phys. Rev. A **93**, 052713 (2016).
[52] S. Jurgilas, A. Chakraborty, C. J. H. Rich, L. Caldwell, H. J. Williams, N. J. Fitch, B. E. Sauer, M. D. Frye, J. M. Hutson, and M. R. Tarbutt, Collisions between ultracold molecules and atoms in a magnetic trap, Phys. Rev. Lett. **126**, 153401 (2021).
[53] H. Werner and P. J. Knowles, An efficient internally contracted multiconfiguration–reference configuration interaction method, J. Chem. Phys. **89**, 5803 (1988).
[54] S. R. Langhoff and E. R. Davidson, Configuration interaction calculations on the nitrogen molecule, Int. J. Quantum Chem. **8**, 61 (1974).
[55] See Supplemental Material at [URL], which includes Refs. [56–62, 64, 65, 67, 69] for details of *ab initio* and CCS calculations and for convergence tests.
[56] C. Makrides, J. Hazra, G. B. Pradhan, A. Petrov, B. K. Kendrick, T. González-Lezana, N. Balakrishnan, and S. Kotochigova, Ultracold chemistry with alkali-metal–rare-earth molecules, Phys. Rev. A **91**, 012708 (2015).
[57] M.-G. Hu, Y. Liu, D. D. Grimes, Y.-W. Lin, A. H. Gheorghe, R. Vexiau, N. Bouloufa-Maafa, O. Dulieu, T. Rosenband, and K.-K. Ni, Direct observation of bimolecular reactions of ultracold KRb molecules, Science **366**, 1111 (2019).
[58] D. E. Woon and T. H. Dunning, Gaussian basis sets for use in correlated molecular calculations. iii. the atoms aluminum through argon, J. Chem. Phys. **98**, 1358 (1993).
[59] H.-J. Werner and *et al.*, MOLPRO, version 2015.1, a package of *ab initio* programs (2015).
[60] M. Gronowski, A. M. Koza, and M. Tomza, Ab initio properties of the NaLi molecule in the $a^3\Sigma^+$ electronic state, Phys. Rev. A **102**, 020801 (2020).
[61] H.-K. Chung, K. Kirby, and J. F. Babb, Theoretical study of the absorption spectra of the sodium dimer, Phys. Rev. A **63**, 032516 (2001).
[62] E. Arimondo, M. Inguscio, and P. Violino, Experimental determinations of the hyperfine structure in the alkali atoms, Rev. Mod. Phys. **49**, 31 (1977).
[63] C. Chin, R. Grimm, P. Julienne, and E. Tiesinga, Feshbach resonances in ultracold gases, Rev. Mod. Phys.

82, 1225 (2010).
[64] R. V. Krems, G. C. Groenenboom, and A. Dalgarno, Electronic interaction anisotropy between atoms in arbitrary angular momentum states, J. Phys. Chem. A **108**, 8941 (2004).
[65] T. Karman, X. Chu, and G. C. Groenenboom, Cold magnetically trapped ^2D_g scandium atoms. i. interaction potential, Phys. Rev. A **90**, 052701 (2014).
[69] T. V. Tscherbul, *Cold Chemistry: Molecular Scattering and Reactivity Near Absolute Zero* (Royal Society of Chemistry, 2018) Chap. 6.
[67] R. N. Zare, *Angular Momentum* (Wiley, 1988).
[68] J. Brown and A. Carrington, *Rotational Spectroscopy of Diatomic Molecules* (Cambridge University Press, 2003).
[69] T. V. Tscherbul, *Cold Chemistry: Molecular Scattering and Reactivity Near Absolute Zero* (Royal Society of Chemistry, 2018) Chap. 6.
[70] N. Balakrishnan, R. C. Forrey, and A. Dalgarno, Quenching of H_2 vibrations in ultracold ^{3}He and ^{4}He collisions, Phys. Rev. Lett. **80**, 3224 (1998).
[71] A. S. Flores, W. Vassen, and S. Knoop, Quantum-state-controlled Penning-ionization reactions between ultracold alkali-metal and metastable helium atoms, Phys. Rev. A **94**, 050701(R) (2016).
[72] J. H. Moore, Investigation of the Wigner spin rule in collisions of N^+ with He, Ne, Ar, N_2, and O_2, Phys. Rev. A **8**, 2359 (1973).
[73] T. V. Tscherbul and R. V. Krems, Controlling electronic spin relaxation of cold molecules with electric fields, Phys. Rev. Lett. **97**, 083201 (2006).
[74] E. Abrahamsson, T. V. Tscherbul, and R. V. Krems, Inelastic collisions of cold polar molecules in nonparallel electric and magnetic fields, J. Chem. Phys. **127**, 044302 (2007).
[75] C. M. Marian, Spin–orbit coupling and intersystem crossing in molecules, WIREs Comput. Mol. Sci. **2**, 187 (2012).
[76] A. O. Lykhin, D. S. Kaliakin, G. E. dePolo, A. A. Kuzubov, and S. A. Varganov, Nonadiabatic transition state theory: Application to intersystem crossings in the active sites of metal-sulfur proteins, Int. J. Quantum Chem. **116**, 750 (2016).
[77] A. O. Lykhin and S. A. Varganov, Intersystem crossing in tunneling regime: $T_1 \rightarrow S_0$ relaxation in thiophosgene, Phys. Chem. Chem. Phys. **22**, 5500 (2020).
[78] T. J. Penfold, E. Gindensperger, C. Daniel, and C. M. Marian, Spin-vibronic mechanism for intersystem crossing, Chem. Rev. **118**, 6975 (2018).
[79] H. Li, A. Kamasah, S. Matsika, and A. G. Suits, Intersystem crossing in the exit channel, Nat. Chem. **11**, 123 (2019).
[80] V. Aquilanti, G. Grossi, and A. Laganà, Hyperspherical diabatic and adiabatic representations for chemical reactions, Chem. Phys. Lett. **93**, 174 (1982).
[81] V. Aquilanti, S. Cavalli, D. De Fazio, A. Volpi, A. Aguilar, X. Giménez, and J. María Lucas, Probabilities for the $F + H_2 \rightarrow HF + H$ reaction by the hyperquantization algorithm: alternative sequential diagonalization schemes, Phys. Chem. Chem. Phys. **1**, 1091 (1999).
[82] K. Nobusada, O. I. Tolstikhin, and H. Nakamura, Quantum mechanical elucidation of reaction mechanisms of heavy-light-heavy systems: Role of potential ridge, J. Chem. Phys. **108**, 8922 (1998).
[83] R. V. Krems and A. Dalgarno, Quantum-mechanical theory of atom-molecule and molecular collisions in a magnetic field: Spin depolarization, J. Chem. Phys. **120**, 2296 (2004).
[84] P. S. Julienne, T. M. Hanna, and Z. Idziaszek, Universal ultracold collision rates for polar molecules of two alkali-metal atoms, Phys. Chem. Chem. Phys. **13**, 19114 (2011).
[85] H. Li, M. Li, C. Makrides, A. Petrov, and S. Kotochigova, Universal scattering of ultracold atoms and molecules in optical potentials, Atoms **7**, 36 (2019).